



## Immobilization of *Aspergillus fumigatus* $\alpha$ -Amylase via Adsorption onto Bentonite/Chitosan for Stability Enhancement

Yandri Yandri <sup>1\*</sup>, Hendri Ropingi <sup>1</sup>, Tati Suhartati <sup>1</sup>, Bambang Irawan <sup>2</sup>, Sutopo Hadi <sup>1</sup>

<sup>1</sup> Department of Chemistry, Faculty of Mathematics and Natural Sciences, University of Lampung, Bandar Lampung 35145, Indonesia.

<sup>2</sup> Department of Biology, Faculty of Mathematics and Natural Sciences, University of Lampung, Bandar Lampung 35145, Indonesia.

### Abstract

Stability enhancement attempted in this study demonstrated that significant improvement in the stability of the  $\alpha$ -amylase isolated from *Aspergillus fumigatus* was achieved by immobilizing the enzyme on a bentonite/chitosan hybrid matrix using the adsorption method. Centrifugation was used to isolate the  $\alpha$ -amylase, which was then refined using  $(\text{NH}_4)_2\text{SO}_4$  salt precipitation and dialysis. The purity of the  $\alpha$ -amylase improved 19.40 times when compared to that of the crude extract. The optimal temperature for free  $\alpha$ -amylase is 50°C, while the optimum temperature for  $\alpha$ -amylase/bentonite/chitosan is 60°C. The  $K_M$  value of  $\alpha$ -amylase/bentonite/chitosan was  $1.69 \pm 0.08$  mg mL<sup>-1</sup> substrate and the  $V_{\max}$  value was  $52.32 \pm 3.29$   $\mu\text{mol mL}^{-1} \text{min}^{-1}$ , whereas for free  $\alpha$ -amylase, the  $K_M$  value of  $2.56 \pm 0.09$  mg mL<sup>-1</sup> substrate and the  $V_{\max}$  value of  $3.78 \pm 0.09$   $\mu\text{mol mL}^{-1} \text{min}^{-1}$  were obtained. The  $\Delta G_i$  value of free  $\alpha$ -amylase is  $102.68 \pm 0.30$  kJ mol<sup>-1</sup> and the  $t_{1/2}$  is  $21.23 \pm 0.23$  min, whereas the  $\Delta G_i$  value of  $\alpha$ -amylase/bentonite/chitosan is  $104.43 \pm 0.00$  kJ mol<sup>-1</sup> and the  $t_{1/2}$  is  $94.29 \pm 0.91$  min. The higher values of  $\Delta G_i$  and  $t_{1/2}$  demonstrated that  $\alpha$ -amylase/bentonite/chitosan has better stability than that of free  $\alpha$ -amylase. Another important finding is that  $\alpha$ -amylase/bentonite/chitosan was able to retain their activity as high as  $47.61 \pm 0.53\%$  after six recycles, indicating that the enzyme has the potential to be used in industry.

### Keywords:

Enzyme Immobilization;  
 $\alpha$ -Amylase;  
Bentonite/Chitosan;  
*Aspergillus fumigatus*.

### Article History:

Received: 21 May 2023  
Revised: 09 August 2023  
Accepted: 02 September 2023  
Available online: 01 October 2023

## 1- Introduction

The  $\alpha$ -amylase (EC 3.2.1.1,  $\alpha$ -1,4-glucan-4-glucanohydrolase) refers to the hydrolase group of enzymes and has been acknowledged as an important class of enzymes in several industries, with continuous growth of application for health and hygiene reasons.  $\alpha$ -Amylase is a crucial enzyme in an array of important industries, including starch conversion, baking industry, detergents, paper, textile industry, production of alcohol for fuel, production of syrups from starch, beverage manufacturing, medicinal, biomedical, and farm waste decomposition [1, 2]. For example, the use of  $\alpha$ -amylase in the baking industry is required to enhance the dough, structure, color, and tenderness of the products. According to Singh et al., amylase accounts for around 25–30% of the global demand for the enzyme utilized in various industries [3]. In 2022, the worldwide market for  $\alpha$ -amylase was reported to reach \$321 million USD, and it is projected to increase by USD 465.5 million by 2032, at a CAGR of 3.8% [4]. The  $\alpha$ -amylase enzyme belongs to the endo-amylase family, which hydrolyzes starch molecules at random, resulted in the production of straight and branched oligosaccharides with different chain lengths through a two-step process. The first step is a fast process in which the starch molecule is randomly broken to produce dextrin, followed by a rapid decline in viscosity. The second step is a comparatively slower process to produce glucose and maltose as the end products.

\* CONTACT: [yandri.as@fmipa.unila.ac.id](mailto:yandri.as@fmipa.unila.ac.id)

DOI: <http://dx.doi.org/10.28991/ESJ-2023-07-05-023>

© 2023 by the authors. Licensee ESJ, Italy. This is an open access article under the terms and conditions of the Creative Commons Attribution (CC-BY) license (<https://creativecommons.org/licenses/by/4.0/>).

The  $\alpha$ -amylase enzymes are widely found in mammals, plants, and microbes. Microbes are the most important sources for industrial sectors for several reasons, such as availability, easy renewability, inexpensive, simple separation, high yields, and requiring less time to produce [5]. Furthermore, enzymes isolated from microbes such as bacteria and fungi are more active and stable than those extracted from plants and mammals [6]. Fungi are popular in the industry because of their ability to rapidly break down biomass, improve resource efficiency, reduce greenhouse gas emissions, and produce appealing flavors, colors, and textures [7]. Fungi from the genus *Aspergillus* are the most important sources for the commercial production of  $\alpha$ -amylase. Some well-known examples are *Aspergillus terreus*, *A. ochraceus*, *A. tamarii* MTCC5152, *A. flavus* AUMC10636, *A. niger*, *A. oryzae*, and *A. fumigatus* [8–14]. Of the various aforementioned sources of  $\alpha$ -amylase, *A. fumigatus* is of particular importance since this fungus is known to have a high ability to endure heat, grow rapidly in a fundamentally nutrient-rich habitat, and require no special nutrition [15]. With respect to the beneficial characteristics of *A. fumigatus*, in this research production of the  $\alpha$ -amylase enzyme from *A. fumigatus* was carried out using the submerged fermentation technique. This method was chosen because it allows more effective interaction between the *A. fumigatus* and the fermentation medium, enhancing the production of  $\alpha$ -amylase as a result.

Regardless of their very important role in industrial processes, enzymes are acknowledged to have some severe practical problems. High temperature conditions may cause a change in the three-dimensional structure of the enzyme proteins from their original (folding) to their denatured (unfolding) form. This structural change leads to decreased catalytic activity, and ultimately the enzyme becomes inactive [16]. Enzymes are sensitive to changes in the pH of their surroundings, causing the enzymes to lose their activity when the pH shifts outside of the optimal range. Furthermore, there are a number of other constraints associated with the utilization of enzymes in industry, including cost, limited availability, solubility in water, which is a particular concern for batch procedures on an industrial scale, contamination by other components that alter the reaction, and limited use to only one run. To alleviate the problem associated with the water solubility of enzymes, one technique that has been progressively explored is the immobilization method, in which the enzyme is attached to a matrix that does not dissolve in the batch, enabling the enzyme to retain its activity. According to Mohamad et al., immobilization techniques may be categorized into two broad categories, generally known as chemical and physical approaches. The two techniques are distinguished based on the interactions between the enzyme and the matrix, in which the physical technique involves non-covalent interactions, whereas the chemical method is characterized by the formation of covalent bonds [17].

Enzyme immobilization methods can improve enzyme stability under mild conditions and allow the enzyme to be reused [18]. The immobilization matrix is heterogeneous materials, making it simple to isolate the products from the reaction mixture [19]. According to Zdarta et al., enzyme immobilization is still widely used in industrial processes due to its benefits, which include high matrix affinity for enzymes, insolubility in reaction processes, biocompatibility properties, the presence of reactive functional groups, availability and less costly, and improved chemical and thermal stability [20]. The matrix used as a support substance for enzyme immobilization is progressively expanding. New materials, also known as hybrid matrices, which combine materials with various characteristics, have lately demonstrated positive results. The goal of this merger is to develop a matrix with superior powers compared to the traditional matrices. Hybrid matrices have numerous benefits, including high mechanical strength, thermal and chemical durability, increased enzyme catalytic efficiency, improved reaction product quality, and enhanced enzyme binding to the matrix [20].

In this study,  $\alpha$ -amylase was isolated and immobilized on a bentonite/chitosan matrix utilizing the adsorption technique. The goal of this research is to develop a hybrid matrix that is simple to prepare, ecologically benign, inexpensive, and reusable for immobilizing  $\alpha$ -amylase to improve the stability of the enzyme, which is a very important characteristic on an industrial scale. A new hybrid matrix composed of bentonite and chitosan and crosslinked with glutaraldehyde, specified as a bentonite/chitosan matrix, was developed and subsequently applied as immobilization support for the  $\alpha$ -amylase enzyme isolated from *A. fumigatus*, using the adsorption method. Bentonite has several advantages, including a large surface area, high adsorption, chemical and bacterial resilience, and mechanical durability [21]. Chitosan, on the other hand, has benefits such as being hydrophilic, biocompatible, and non-toxic [22]. The adsorption technique, according to Mohamad et al., has the benefit of being easy and simple [17]. The formation of non-covalent interactions, such as hydrogen bonds, Van der Waals forces, affinity effects, ionic bonds, and hydrophilicity, is a distinguishing trait of the adsorption technique. Furthermore, because the matrix used can be readily separated if the enzyme activity is lost, this technique is ideal for lowering manufacturing costs. Once separated, the matrix can be repurposed by binding to a new enzyme. Tiarsa et al. found that using a hybrid matrix of bentonite and chitin increased the thermal durability of the  $\alpha$ -amylase from *A. fumigatus* by 3.8 times compared to that of the free enzyme [23]. Meanwhile, when compared to free enzymes, the use of bentonite alone only increased thermal durability by 2.9 times [24]. Previous workers reported that the use of a hybrid matrix of zeolite and chitosan boosted the thermal resistance of the *A. fumigatus*  $\alpha$ -amylase by 4.65 times when compared to the free enzyme [25].

## 2- Materials and Methods

### 2-1- Materials

The *A. fumigatus* was acquired from the Microbiology Laboratory, Department of Biology, University of Lampung. Bentonite ( $\text{Al}_2\text{O}_3 \cdot 4\text{SiO}_2 \cdot \text{H}_2\text{O}$ ), chitosan (deacetylated chitin, poly(D-glucosamine)) with a deacetylation degree of 75%, and glutaraldehyde solution (-50 wt.% in  $\text{H}_2\text{O}$ ) were purchased from Sigma Aldrich™. All of the materials used are of pro analysis.

## 2-2- Production and Isolation of $\alpha$ -Amylase from *A. fumigatus*

The fermentation media consisted of  $(\text{NH}_4)_2\text{SO}_4$  3.5 grams,  $\text{KH}_2\text{PO}_4$  5 grams,  $\text{MgSO}_4 \cdot 7\text{H}_2\text{O}$  0.75 grams, urea 0.75 grams,  $\text{CaCl}_2$  0.75 grams,  $\text{FeSO}_4 \cdot 7\text{H}_2\text{O}$  0.0125 grams,  $\text{ZnSO}_4 \cdot 7\text{H}_2\text{O}$  0.0035 grams,  $\text{CoCl}_2$  0.005 grams, corn starch 1.875 grams, and peptone 1.875 grams were dissolved in 250 mL of 0.05 M phosphate buffer with the pH of 6.5. The fermentation was carried out for 112 hours at 32°C using the submerged fermentation technique. The  $\alpha$ -amylase crude extract was isolated by centrifugation at 5000 rpm for 15-20 minutes [25]. The research's flowchart is displayed in Figure 1.

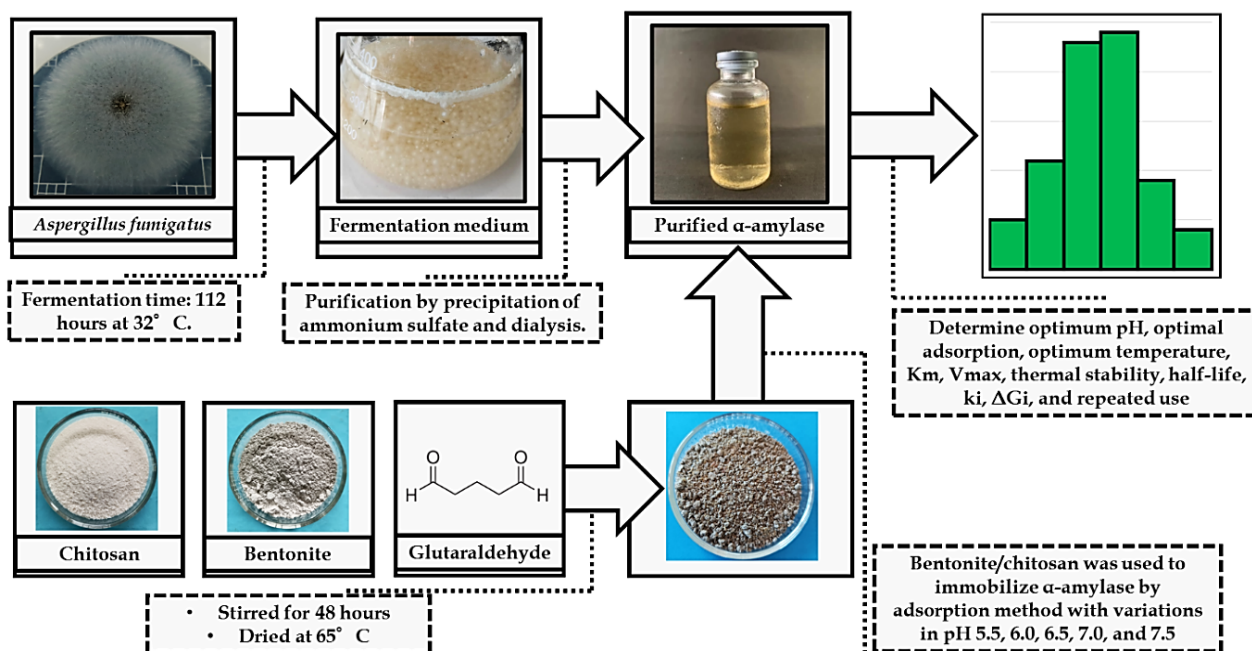


Figure 1. Flowchart of the research

## 2-3- Purification of $\alpha$ -Amylase

While agitating with a magnetic agitator, enzyme crude extract was steadily supplied with  $(\text{NH}_4)_2\text{SO}_4$  salt. Cold centrifugation at 5000 rpm for 15 minutes was conducted to separate the enzyme precipitate produced in each saturated portion of ammonium sulfate from the filtrate. The separated enzyme was placed in a cellophane bag and subjected to 24 hours dialysis treatment at 4°C using 0.01 M phosphate buffer pH 6.5. During dialysis, the buffer was replaced every 4-6 hours to decrease the concentration of ions in the cellophane [25, 26].

## 2-4- Activity Test and Protein Content Determination

The activity of the  $\alpha$ -amylase investigated was determined using the iodine and dinitrosalicylic acid methods. The iodine method is a useful and practical method to follow a decrease in the quantity of substrate (starch) after the hydrolysis process [27], and the dinitrosalicylic acid method is a common method to determine the concentration of glucose resulting from the starch hydrolysis process [28]. The Lowry technique was used to measure enzyme protein levels [29].

## 2-5- Determination of the Optimum pH

To find out at what pH the  $\alpha$ -amylase exhibited the highest activity, the activity tests for the enzyme sample produced from dialysis was conducted at varied pH levels of 5.5; 6.0; 6.5; 7.0; and 7.5. The pH at which the enzyme displayed the highest activity was taken as determined.

## 2-6- Preparation of Bentonite/chitosan

A mass of 7.5 g of chitosan was dissolved in 100 mL of 1% acetic acid solution followed by addition of 5 mL of 1 M NaOH and 300 mL of distilled water. Into dissolved chitosan a mass of 7.5 g of bentonite was added and the mixture was mixed for 24 hours at 120 rpm using an incubator shaker. After the completion of the mixing, an aliquot of 7.5 mL of 0.4% (v/v) glutaraldehyde was added. The mixture was then mixed again for 24 hours at 120 rpm using an incubator shaker. The precipitate formed was then separated from liquid part and then dried at 65°C, and finally characterized using FTIR to determine the chemical groups of the resulting bentonite/chitosan combination [25].

### 2-7- Determination of Optimal Conditions for Formation of $\alpha$ -Amylase/bentonite/chitosan ( $\alpha$ -A/Bt/Ct)

A mass of 0.2 gram of bentonite/chitosan was stabilized with buffer solutions with varied pHs of 5.5; 6.0; 6.5; 7.0; and 7.5, and then a mixture of 0.5 mL of purified enzyme with 0.5 mL of buffer solution was added into bentonite/chitosan. The mixture was then centrifuged to separate. The resulting supernatant was then analyzed for activity to identify which enzymes were not adsorbed. The activity of the precipitate was determined to identify which enzymes were absorbed and attached to bentonite/chitosan. The optimal pH state is described as the activity that gives the highest activity [25].

### 2-8- Immobilization of the $\alpha$ -Amylase on Bentonite/chitosan

0.2 gram of bentonite/chitosan stabilized buffer solution with optimum pH was mixed with 0.5 mL of purified enzyme and 0.5 mL of buffer solution with optimum pH. The mixture was then centrifuged to separate the supernatant from the precipitate. The precipitate was then reacted with starch (substrate).

### 2-9- Determination of Optimum Temperature

In order to hydrolyse starch into glucose,  $\alpha$ -amylase enzymes require elevated temperatures in industry. This is because at high temperatures significant interaction between the enzyme and the substrate takes place rapidly. In this study, the free  $\alpha$ -amylase and  $\alpha$ -A/Bt/Ct were subjected to incubation treatment at temperatures in the range of 45 to 80°C with 5°C variation in order to determine the optimum temperature for the enzyme.

### 2-10- Determination of Chemical Kinetics

The Michaelis-Menten constant ( $K_M$ ) and maximum rate of reaction ( $V_{max}$ ) were calculated from the activities of free  $\alpha$ -amylase and  $\alpha$ -A/Bt/Ct against different substrate concentrations of 0.1, 0.2, 0.4, 0.6, and 0.8%, at their optimum temperatures. Lineweaver-Burk curve was produced by plotting the rates of the reaction and the concentrations of the substrate. The Lineweaver-Burk equation was used to calculate the  $K_M$  and  $V_{max}$  values shown in Equation 1.

$$\frac{1}{v} = \frac{1}{V_{max}} + \frac{K_M}{V_{max}} \times \frac{1}{[S]} \quad (1)$$

where  $K_M$  is the Michaelis constant;  $V_{max}$  is the maximum reaction rate;  $v$  is the initial reaction rate; and  $[S]$  is the substrate concentration.

### 2-11- Determination of Thermal Stability

Enzyme stability at high temperatures is a major issue because it pertains to enzyme denaturation. The goal of temperature stability testing is to identify the immobilized enzyme's resilience to free  $\alpha$ -amylase. This technique was used to evaluate the residual activity of free  $\alpha$ -amylase and  $\alpha$ -A/Bt/Ct by changing the incubation duration at 60°C. Incubation times was changed from 0 to 10, 20, 30, 40, 50, 60, 70, and 80 minutes. The residual activity was calculated using Equation 2.

$$\text{Residual activity (\%)} = \frac{E_i}{E_o} \times 100\% \quad (2)$$

where  $E_o$  is the residual activity at  $t_o$  and  $E_i$  is the residual activity at  $t_i$  [30].

### 2-12- Determination of the Value of $t_{1/2}$ , $k_i$ , and $\Delta G_i$

The values of the thermal inactivation rate constant ( $k_i$ ) and  $t_{1/2}$  were determined based on the equation of the first order inactivation rate ( $k_i$ ) between the residual activity of the enzyme on  $t_o$  ( $[E]_o$ ) and the activity of the remaining enzyme on  $t_i$  ( $[E]_i$ ) (Equation 3).

$$\ln \left( \frac{E_i}{E_o} \right) = -k_i \times t_i \quad (3)$$

Equation 4 can be used to determine the free energy changes as a consequence of denaturation ( $\Delta G_i$ ) of free  $\alpha$ -amylase and  $\alpha$ -A/Bt/Ct obtained from the thermodynamic equation.

$$\Delta G_i = -RT \ln \frac{k_i \cdot h}{k_b \cdot T} \quad (4)$$

where  $R$  is the ideal gas constant (8.315 J K<sup>-1</sup> mol<sup>-1</sup>),  $T$  is the absolute temperature (K),  $k_i$  is the thermal inactivation rate constant,  $h$  is Planck's constant (6.625 × 10<sup>-34</sup> J sec), and  $k_b$  is the constant Boltzman (1.381 × 10<sup>-23</sup> J K<sup>-1</sup>) [31].

### 2-13- Repeated Use

In this work, the  $\alpha$ -A/Bt/Ct was tested 6 times. After each use, the used  $\alpha$ -A/Bt/Ct was washed with an optimal pH solution and centrifuged. The immobilized enzyme precipitate was then reacted with the new substrate. The residual activity (%) of immobilized enzymes was then evaluated and compared before and after 6 repeats [25].

## 2-14-Statistical Analysis

Sample measurements were evaluated twice ( $n=2$ ), and the results are shown in mean standard variation (SD). As a result, in addition to ANOVA, the potential of significant variations between samples was tested using the t-test (Paired Two Sample for Means). The results are thought to be significant at  $p$  0.05 in order to deny the null hypothesis.

## 3- Results and Discussion

### 3-1- Isolation and Purification of the $\alpha$ -Amylase from *A. fumigatus*

The  $\alpha$ -amylase crude extract was obtained by centrifuging the fermented product at 5000 rpm for 15-20 minutes. The crude extract was found to have unit activity of  $58.81 \text{ U mL}^{-1}$  and a specific activity of  $280.05 \text{ U mg}^{-1}$ . The crude extract was then purified using the  $(\text{NH}_4)_2\text{SO}_4$  precipitation method and dialysis. With  $(\text{NH}_4)_2\text{SO}_4$ , the precipitation pattern is 0-20% and 20-85% [17]. Figure 2 depicts the connection between  $(\text{NH}_4)_2\text{SO}_4$  percent concentration and enzyme specific activity. The selection of the 20-85% portion is to reduce wasted enzyme, so that the maximum enzyme is received. The 20-85% fraction was found to have a unit activity of  $389.82 \text{ U mL}^{-1}$  and a specific activity of  $1499.30 \text{ U mg}^{-1}$ . As a result, the purity level of the 20-85% portion is 5.35 times than that of the crude extract. Table 1 shows the findings of the purification stage of the  $\alpha$ -amylase investigated.

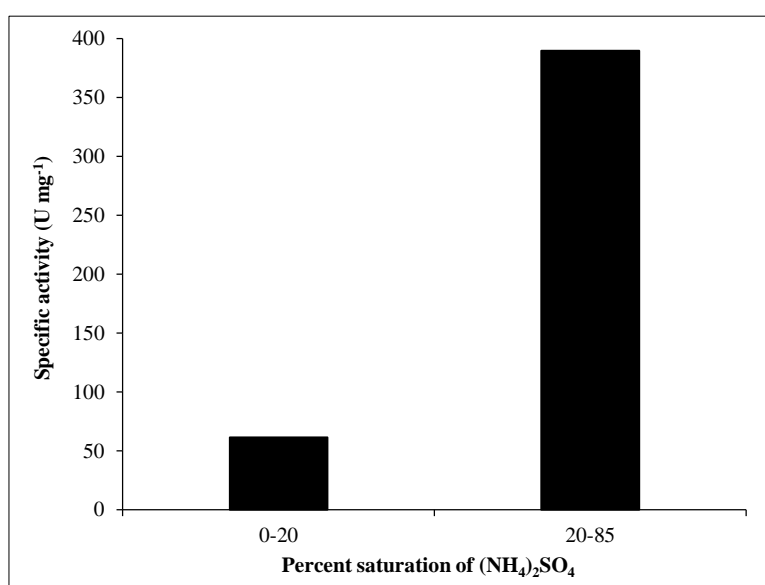


Figure 2. Fractionation scheme using  $(\text{NH}_4)_2\text{SO}_4$

Table 1. Table of  $\alpha$ -amylase purification from *A. fumigatus*

Stage	Volume (mL)	Unit activity ( $\text{U mL}^{-1}$ )	Protein content ( $\text{mg mL}^{-1}$ )	Specific activity ( $\text{U mg}^{-1}$ )	Total activity (U)	Purity level	Recovery (%)
Enzyme crude extract	2000	58.81	0.21	280.05	117620.00	1.00	100.00
Fraction of $(\text{NH}_4)_2\text{SO}_4$ (20-85%)	70	389.82	0.26	1499.30	27287.40	5.35	23.20
Dialysis	100	271.58	0.05	5431.60	27158.00	19.40	23.10

Dialysis for 24 hours with 0.01 M phosphate buffer pH 6.5 removes the  $(\text{NH}_4)_2\text{SO}_4$  salt at a fraction of 20-85%. Because of differences in buffer concentrations,  $(\text{NH}_4)_2\text{SO}_4$  salts will pass through the semipermeable membrane. After dialysis, the enzymes have a greater purity rise than that of the crude extract. This is evidenced by the dialyzed enzyme's enhanced specific activity of  $5431.60 \text{ U mg}^{-1}$  when compared to the crude enzyme extract. When compared to the crude extract, the purified enzyme has a purity level of 19.40 times. According to Table 1, the protein concentration of each purification procedure dropped, indicating that the protein impurities has been vanished. In earlier investigations, the purity of the dialyzed  $\alpha$ -amylase from *A. fumigatus* was 10 and 14.5 times [24, 25]. In this regard, the results of this study indicate that the purity and catalytic activity of  $\alpha$ -amylase from *A. fumigatus* significantly increased compared to those reported in previous studies.

### 3-2- Determination of the Optimum pH

The optimum pH for the enzyme investigated was determined by conducting experiments at varied pHs, with the results as shown in Figure 3. As can be seen in Figure 3, the highest activity was exhibited by the enzyme at pH = 6.5, and slightly declines when the conditions were shifted to neutral condition, followed by quite significant decline at

alkaline conditions, suggesting that the enzyme is unstable in alkaline conditions. Several workers also reported the optimum pH at acidic range for  $\alpha$ -amylase isolated from different sources. In previous research, Planchot & Colonna reported the optimum pH of 5.5 for the  $\alpha$ -amylase isolated from *A. fumigatus* (*Aspergillus* sp. K-27) is 5.5 [32]. This optimum pH is the same for  $\alpha$ -amylase isolated from *A. fumigatus* [33], while the optimum pH of 6.0 was reported by Akhter et al. [34] for  $\alpha$ -amylase isolated from *A. fumigatus* Fresenius. The agreement between the optimum pH observed in this study and those reported by others confirm that  $\alpha$ -amylase enzyme from *A. fumigatus* tends to work most effectively at in acidic conditions, which also implies that the enzyme is stable in acidic environments.

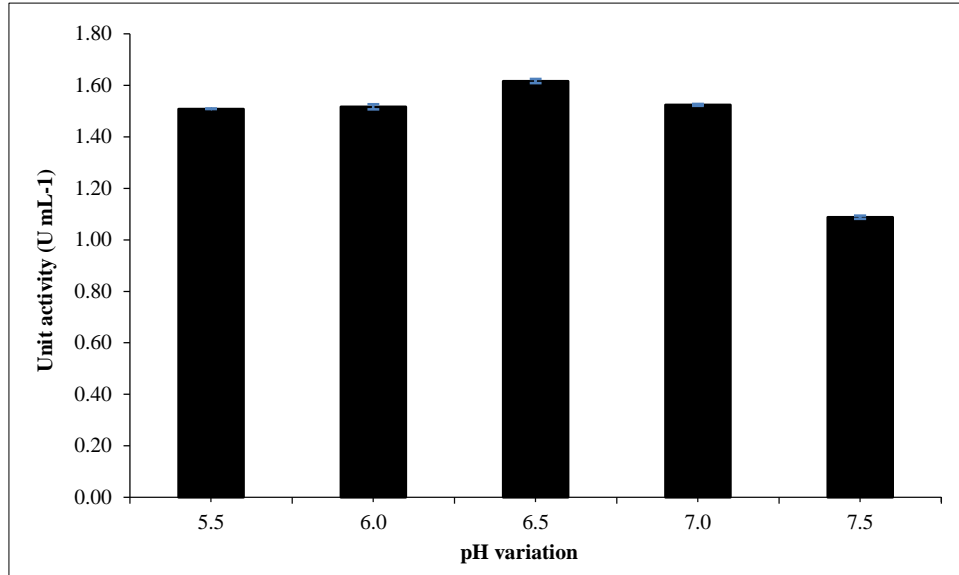


**Figure 3.** Relationship between pH variations and the activity of the  $\alpha$ -amylase units from *A. fumigatus* (mean  $\pm$  SD; n = 2; p <0.05)

### 3-3-Fourier Transform Infrared (FTIR) Spectrometry Analysis of Bentonite/chitosan

To identify functional groups of the samples, bentonite, chitosan, and bentonite/chitosan were characterized using FT-IR technique, and the resulted spectra are compiled in Figure 4. The FTIR spectrum of is characterized by the presence of absorption bands in the range 3,631.96 to 3,448.72  $\text{cm}^{-1}$ , assigned to stretching vibration of H-O-H weakly bound to the Si-O surface [35]. The H<sub>2</sub>O bending vibration is indicated by the absorption band at 1,637.56  $\text{cm}^{-1}$  [36]. The absorption bands 1045.42, 918.12, and 798.53  $\text{cm}^{-1}$  are associated with Si-O-Si stretching, OH bending, and free Si broadening [37, 38]. The band at 623.01  $\text{cm}^{-1}$  is a mix of the Al-O and Si-O vibrational fields [28]. The absorption bands at 524.64 and 466.77  $\text{cm}^{-1}$  represent bending modes of Si-O-Al and Si-O-Si [38]. In the spectrum of chitosan, the existence of CH<sub>3</sub>, CH<sub>2</sub>, CH, NH<sub>2</sub>, together with primary and secondary OH groups attached to the pyranose ring, as well as glycosidic bonds is indicated by absorption peak in the range 1,423.47-617.22  $\text{cm}^{-1}$ . Furthermore, the existence of C=O in the NHC(=O)CH<sub>3</sub> and C-H groups in the pyranose ring is indicated by the absorption bands at 1,656.85 and 2,879.72  $\text{cm}^{-1}$  [39]. The vibrational strain of the intermolecular and intermolecular hydrogen bonds of the NH<sub>2</sub> and O-H groups is indicated by a wide band at around 3,448.72  $\text{cm}^{-1}$  [40].

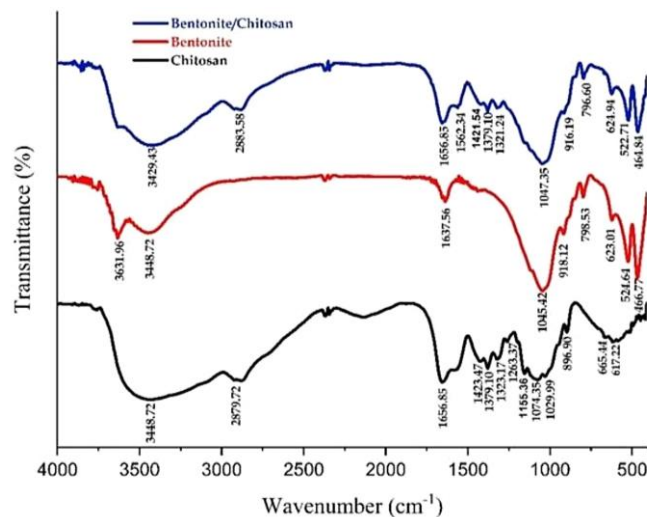


**Figure 4.** FTIR spectra of bentonite, chitosan, and bentonite/chitosan

The FTIR spectrum of bentonite/chitosan reveals a mixture of bentonite and chitosan groups. A slightly shift of the absorption band in the wave number range of 1047.35-464.84  $\text{cm}^{-1}$  was observed. This region is assigned to stretching region of Si-O-Si, the bending of O-H, the widening of free Si, the combining out of the Al-O and Si-O vibrational fields, and the bending modes of Si-O-Al and Si-O-Si. The absorption band at 1423.47  $\text{cm}^{-1}$  shifted to 1421.54  $\text{cm}^{-1}$ , and the absorption band at 1323.47  $\text{cm}^{-1}$  shifted to 1321.24  $\text{cm}^{-1}$ , both are associated to  $\text{CH}_2$  in the  $\text{CH}_2\text{OH}$  group and C-H in the pyranose ring. Meanwhile, the position of absorption band representing  $\text{CH}_3$  group of the  $\text{NHCOCH}_3$  remains unchanged (1,379.10  $\text{cm}^{-1}$ ), and the same is true for the position of the C=O group. The  $\text{NH}_2$  and O-H groups are responsible for the shift from 3,448.72  $\text{cm}^{-1}$  to 3,429.43  $\text{cm}^{-1}$ . This shift is due to overlapping as a result of formation of bentonite and chitosan composite. After merging with chitosan, the stretching vibration of the H-O-H, which is loosely bound to the Si-O surface of bentonite, is no longer evident. This is due to the drying of the material during the synthesis process.

### 3-4-Determination of Optimal Adsorption Conditions for $\alpha$ -Amylase with Bentonite/chitosan

pH is an important parameter in immobilizing enzymes by adsorption because it influences the binding parameters between the enzymes and the matrix. Therefore, the performance of the enzyme at different pHs can be used as a base to determine the optimum parameters for the adsorption of  $\alpha$ -amylase on bentonite-chitosan. Figure 5 demonstrates the activity of the  $\alpha$ -amylase in the adsorption process at different pH levels. According to Figure 5, the bound enzyme exhibited the greatest activity at pH 6.0. In previous study, it was reported that  $\alpha$ -amylase from *A. fumigatus* was optimally attached to bentonite as a matrix at pH 7.5 [24]. Electrostatic contact between the positive charge of bentonite/chitosan and the negative charge of the enzyme at pH 7.5 is suggested to make the enzyme is adsorbed more effectively [23]. However, at neutral pH, the activity of the  $\alpha$ -amylase is insufficient, resulting in losses due to reduced enzymatic activity. The binding rate at pH 6.0 was  $5.37 \pm 0.57$  times that at pH 7.5. The pH of 6.0 is better because it is within the highest working range for the enzyme, so there is no risk of a decline in its catalytic activity.

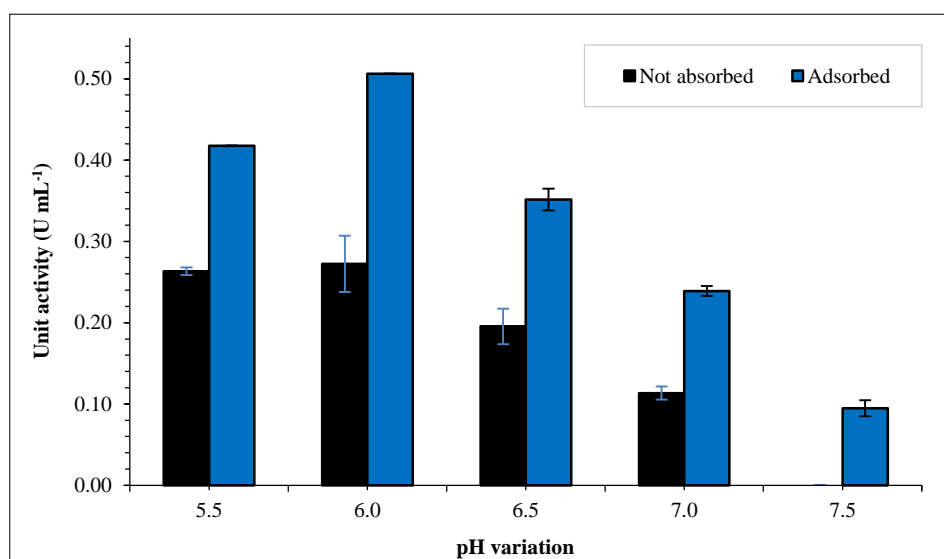


**Figure 5.** Correlation between pH variation and adsorption activity of  $\alpha$ -amylase from *A. fumigatus* (mean  $\pm$  SD; n = 2; p < 0.05)

The optimum pH for contact of the enzyme with the bentonite/chitosan matrix after is 6.0. In previous study, it was found that at pH 6.0, the free enzymes exhibited greater activity than that of the enzymes adsorbed on bentonite [24]. In the work by Agustine et al., it was reported that the use of core-shell structured aniline formaldehyde crosslinked polyaniline magnetic nanocomposite is able to improve the performance of the immobilized  $\alpha$ -amylase enzyme in alkaline conditions compared to that of free enzyme [41]. In another study it was reported that at pH 4.5, chitosan mixed with zeolite binds  $\alpha$ -amylase from *A. fumigatus* optimally [25]. In an acidic environment, the  $\alpha$ -amylase from *A. fumigatus* is more active than in an alkaline environment. Wang et al. found similar outcomes when using chitosan mixed with halosite nanotubes to immobilize laccase from *Trametes versicolor*, with a maximum adsorption state at an acidic pH (pH 5), and a drastic decrease in adsorption at a more alkaline pH [42]. It has been demonstrated that combining bentonite/chitosan can boost the amount of adsorbed enzymes in the acidic area. This is due to chitosan's unique property, which is that under acidic circumstances, the  $\text{NH}_2$  group in the linear chain changes to  $\text{NH}_3$  [43]. Acidic pH conditions can support the association of negatively charged enzyme groups with positively charged chitosan groups [44, 45].

### 3-5-Determination of Optimal Temperature Conditions

An optimal temperature is required in the reaction process between the enzyme and the substrate in to produce the highest yield. The active site of the enzyme will open and interact well with the substrate at the optimum temperature,

resulting in an excellent enzyme-substrate complex. Figure 6 depicts the impact of temperatures on the activity of free  $\alpha$ -amylase and  $\alpha$ -A/Bt/Ct, demonstrating that the optimum temperature for free  $\alpha$ -amylase is 50°C while for the immobilized enzyme, the optimum temperature of 60°C was observed. In addition to higher optimum temperature, the remaining activity of  $\alpha$ -A/Bt/Ct was much higher than that of free  $\alpha$ -amylase at temperatures ranging from 60°C to 80°C. Previous workers suggested that the  $\alpha$ -amylase is protected by a matrix on which it is immobilized, which results in optimum temperature shifts to higher value and higher activity [46].

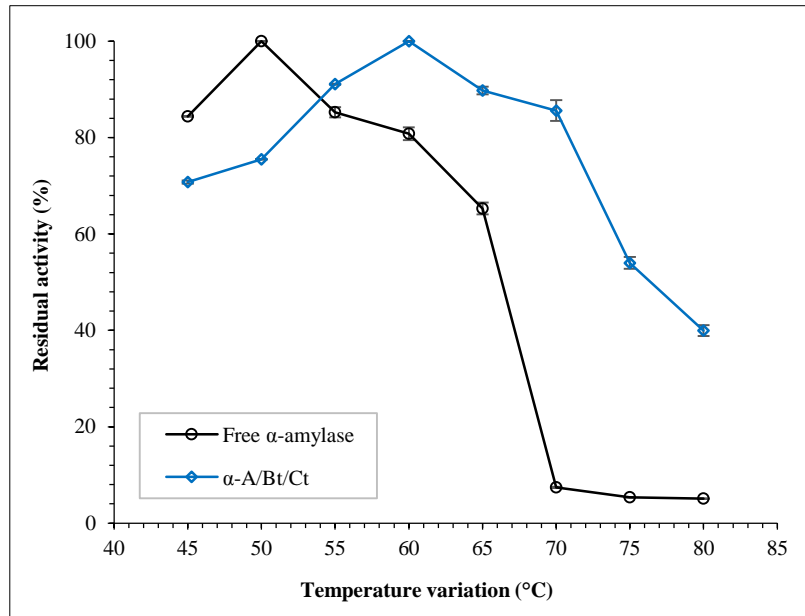


**Figure 6.** Correlation between temperature variations and free  $\alpha$ -amylase and  $\alpha$ -A/Bt/Ct activities (mean  $\pm$  SD; n = 2; p < 0.05)

The change in optimum temperature results in a shift in the optimum conditions for the formation of the enzyme-substrate complex. Table 2 shows the optimum temperatures for  $\alpha$ -amylase in free state and immobilized on various matrices used, demonstrating the influence of the matrices used on optimum temperature of the enzyme. According to Bodakowska-Boczniewicz and Garncarek, the use of a matrix of chitosan microspheres triggered with glutaraldehyde can induce the optimum temperature change of the *Penicillium decumbens* naringinase from 40 to 70°C [47]. The use of gellan-based hydrogel particles to immobilize  $\alpha$ -amylase from porcine pancreatic was able to increase the optimal temperature from 35 to 60°C [48]. According to Ahmed et al. the use of alginate beads was able to increase the optimal temperature of  $\alpha$ -amylase isolated from *A. terreus* from 50 to 60°C [49].

**Table 2.** Optimal temperatures of free and immobilized  $\alpha$ -amylase in different matrices

Host	Matrix	Optimal temperature (°C)		Reference
		Free $\alpha$ -amylase	Immobilized $\alpha$ -amylase	
<i>A. fumigatus</i>	Bentonite	55	70	[24]
<i>A. fumigatus</i>	Zeolite	50	60	[50]
<i>A. terreus</i>	alginate beads	50	60	[49]
porcine pancreatic	gellan-based hydrogel particles	35	70	[48]
<i>A. fumigatus</i>	Zeolite/chitosan	50	55	[25]
<i>A. fumigatus</i>	Bentonite/chitin	55	60	[23]
<i>A. fumigatus</i>	Bentonite/chitosan	50	60	This study

### 3-6-Determination of Chemical Kinetics

The determination of  $K_M$  and  $V_{max}$  attempts to determine the maximum reaction rate by determining the concentration of the substrate. The  $K_M$  and  $V_{max}$  were determined by varying the concentrations of the substrate. Figure 7 shows the Lineweaver-Burk equation graph used to calculate the  $K_M$  and  $V_{max}$  values. Table 3 shows the results of calculating the  $K_M$  and  $V_{max}$  values for free  $\alpha$ -amylase, as well as the results of immobilization in the different matrices used.

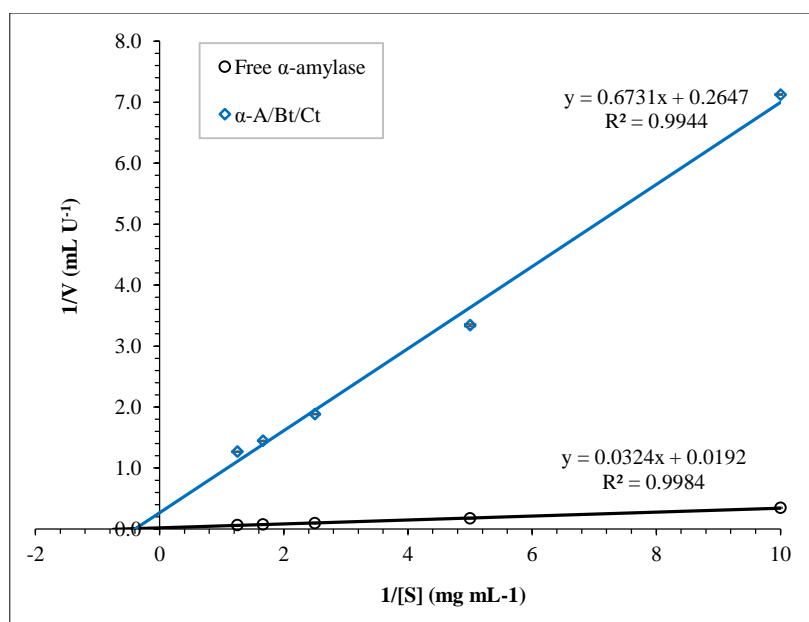


**Figure 7.** Lineweaver-Burk plot of free  $\alpha$ -amylase and  $\alpha$ -A/Bt/Ct from *A. fumigatus* (mean  $\pm$  SD; n = 2; p < 0.05)

In Table 3,  $V_{\max}$  value decreased from  $52.32 \pm 3.29$  to  $3.78 \pm 0.09 \mu\text{mol mL}^{-1} \text{min}^{-1}$ . The  $V_{\max}$  value of free  $\alpha$ -amylase was greater than that of immobilized enzyme, suggesting that the free enzyme can hydrolyze a wider range of substrates.  $K_M$  value increased from  $1.69 \pm 0.08$  to  $2.56 \pm 0.09 \text{ mg mL}^{-1}$  substrate. The high  $K_M$  value is owing to the reduced affinity of the enzyme toward the substrate. The same findings were achieved by Nazarova et al. who used a ceramic membrane to immobilize  $\alpha$ -amylase from *Bacillus subtilis*, resulting in a decrease in  $V_{\max}$  and an increase in  $K_M$  [51]. According to Kaushal et al. the catalase immobilized with bentonite and bentonite/chitosan displayed greater  $K_M$  value and a lower  $V_{\max}$  value than those of the unimmobilized enzyme [52]. Because the matrix utilized displaced the substrate toward the active site, the  $V_{\max}$  and  $K_M$  values are altered. As a result, the substrate moving to the active site is obstructed by the matrix during the reaction process, reducing its accessibility relative to the free enzyme. According to Califano and Costantini (2020), the structural changes that occur when the enzyme is protected by the matrix is due to non-covalent bonds between the enzyme and the matrix [53, 54].

**Table 3.**  $K_M$  and  $V_{\max}$  values of free and immobilized  $\alpha$ -amylase in different matrices

Matrix Type	$K_M$		$V_{\max}$		Ref.
	Free $\alpha$ -amylase	Immobilized $\alpha$ -amylase	Free $\alpha$ -amylase	Immobilized $\alpha$ -amylase	
Bentonite	$3.04 \pm 1.04 \text{ mg mL}^{-1}$ substrate	$8.31 \pm 2.67 \text{ mg mL}^{-1}$ substrate	$10.90 \pm 1.89 \mu\text{mol mL}^{-1} \text{min}^{-1}$	$1.44 \pm 0.30 \mu\text{mol mL}^{-1} \text{min}^{-1}$	[24]
Zeolite	$3.478 \pm 0.271 \text{ mg mL}^{-1}$ substrate	$11.685 \pm 0.183 \text{ mg mL}^{-1}$ substrate	$2.211 \pm 0.096 \mu\text{mol mL}^{-1} \text{min}^{-1}$	$1.406 \pm 0.049 \mu\text{mol mL}^{-1} \text{min}^{-1}$	[50]
TiO <sub>2</sub> /lignin hybrid	11.04 mM	15.03 mM	920 U/mg	855 U/mg	[46]
Chitosan	$1.63 \text{ mg mL}^{-1}$	$3.51 \text{ mg mL}^{-1}$	$39.68 \mu\text{mole mL}^{-1} \text{min}^{-1}$	$7.05 \mu\text{mole mL}^{-1} \text{min}^{-1}$	[55]
ceramic membrane	$4.3 \text{ mg mL}^{-1}$	$4.7 \text{ mg mL}^{-1}$	$61 (\text{mg}_{\text{enzyme}} \text{min})^{-1}$	$45 (\text{mg}_{\text{enzyme}} \text{min})^{-1}$	
Zeolite/chitosan	$3.478 \pm 0.271 \text{ mg mL}^{-1}$ substrate	$12.051 \pm 4.949 \text{ mg mL}^{-1}$ substrate	$2.211 \pm 0.096 \mu\text{mol mL}^{-1} \text{min}^{-1}$	$1.602 \pm 0.576 \mu\text{mol mL}^{-1} \text{min}^{-1}$	[25]
Bentonite/chitin	$3.04 \pm 1.04 \text{ mg mL}^{-1}$ substrate	$11.57 \pm 0.76 \text{ mg mL}^{-1}$ substrate	$10.90 \pm 1.89 \mu\text{mol mL}^{-1} \text{min}^{-1}$	$3.37 \pm 0.12 \mu\text{mol mL}^{-1} \text{min}^{-1}$	[23]
Bentonite/chitosan	$1.69 \pm 0.08 \text{ mg mL}^{-1}$ substrate	$2.56 \pm 0.09 \text{ mg mL}^{-1}$ substrate	$52.32 \pm 3.29 \mu\text{mol mL}^{-1} \text{min}^{-1}$	$3.78 \pm 0.09 \mu\text{mol mL}^{-1} \text{min}^{-1}$	This study

### 3-7-Determination of Thermal Stability

Thermal stability was determined by incubating free  $\alpha$ -amylase and  $\alpha$ -A/Bt/Ct at  $60^\circ\text{C}$  for 0, 10, 20, 30, 40, 50, 60, 70, and 80 minutes. Figure 8 depicts the thermal stability of  $\alpha$ -A/Bt/Ct, which is more stable than free  $\alpha$ -amylase. The residual activity of free  $\alpha$ -amylase was  $7.42 \pm 0.02\%$ , whereas  $\alpha$ -A/Bt/Ct has the residual activity of  $59.61 \pm 0.43\%$ .  $\alpha$ -A/Bt/Ct demonstrated greater residual activity than free  $\alpha$ -amylase during 10 to 80 minutes of incubation. This is because the bentonite/chitosan matrix can protect the  $\alpha$ -amylase, preventing denaturation of the enzyme [56].

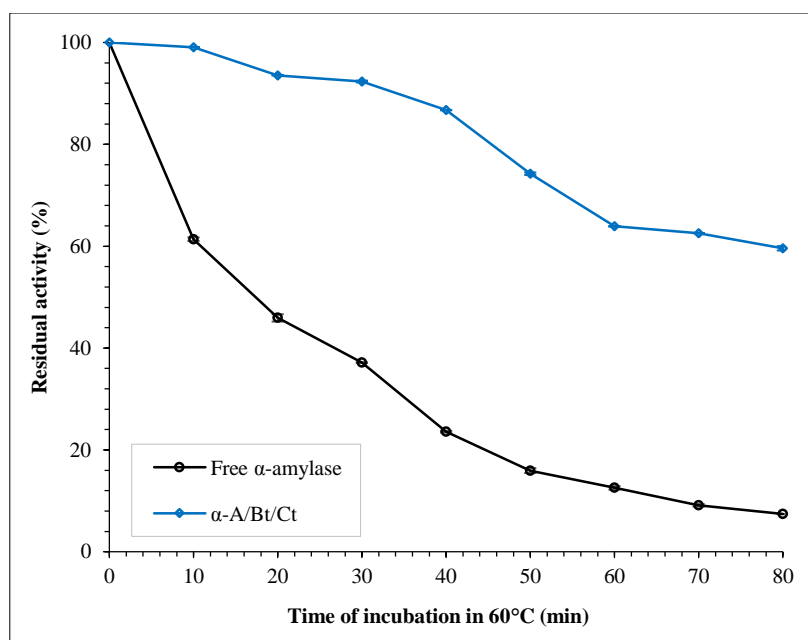


**Figure 8.** Thermal stability of free  $\alpha$ -amylase and  $\alpha$ -A/Bt/Ct from *A. fumigatus* (mean  $\pm$  SD; n = 2; p <0.05)

The hydrophilic parts of the enzymes are located on the exterior of the enzymes. In the adsorption technique, positively charged hydrophilic moieties such as lysine, histidine, and arginine can interact with bentonite groups such as Si-O-Si, O-H, Al-O, Si, and Si-O-Al via non-covalent bonds such as hydrogen bonds, hydrophobic interactions, electrostatic interactions, and Van der Waals forces. The oxygen from the bentonite will form a hydrogen connection with the  $\text{NH}_3^+$  group on the lysine, histidine, and arginine. Furthermore, the excess of -OH groups in chitosan can enhance associations with enzymes that contain  $\text{NH}_2$  groups on lysine, histidine, and arginine residues. Table 4 displays the findings of immobilization of  $\alpha$ -amylase obtained from *A. fumigatus* on different matrices and the results of determining the thermal durability for free  $\alpha$ -amylase. Table 4 demonstrates that, when compared to the other matrices, the combined bentonite/chitosan matrix has the highest ratio between enzymes that are immobilized and those of free enzyme. The binding of enzymes to the matrix leads to better improvement of the stability when hybrid matrices were used compared to the single conventional matrices (bentonite and zeolite), the use of hybrid matrices results in a higher ratio. This is because the hybrid matrix has thermal and chemical stability, mechanical resistance, and make the enzymes bound to the matrix more stable [20].

**Table 4.** Thermal stability values of free and immobilized  $\alpha$ -amylase from *A. fumigatus* in different matrices

Matrix	Residual activity (%)		Ratio	Reference
	Free $\alpha$ -amylase	Immobilized $\alpha$ -amylase		
Bentonite	29	56	1,93	[24]
Zeolite	21.50 $\pm$ 0.11*	49.18 $\pm$ 0.07*	2.29 $\pm$ 0.01*	[50]
Zeolite/chitosan	21.50	72.28	3.36	[25]
Bentonite/chitin	30	72	2,40	[23]
Bentonite/chitosan	7.42 $\pm$ 0.02*	59.61 $\pm$ 0,43*	8.04 $\pm$ 0.04*	This study

\* (mean  $\pm$  SD; n = 2; p <0.05)

### 3-8-Determination of the Value of $t_{1/2}$ , $k_i$ , and $\Delta G_i$

The first order thermal deactivation rate was graphed using the measured thermal stability of the enzyme. Figure 9 displays the curve of  $\ln(E_i/E_0)$  for free  $\alpha$ -amylase and  $\alpha$ -A/Bt/Ct. The slope of the line in Figure 9 represents the rate constant of thermal inactivation ( $k_i$ ) and is used to determine the half-life ( $t_{1/2}$ ) and the free energy conversion due to denaturation ( $\Delta G_i$ ). Table 5 displays the  $t_{1/2}$  and  $\Delta G_i$  values for free and immobilized enzyme. The data in Figure 9 demonstrate that free  $\alpha$ -amylase has a greater  $k_i$  value than that of  $\alpha$ -A/Bt/Ct. When compared to free  $\alpha$ -amylase, the denaturation rate constant ( $k_i$ ) of immobilized enzyme is smaller, suggesting a slower rate of enzyme denaturation.

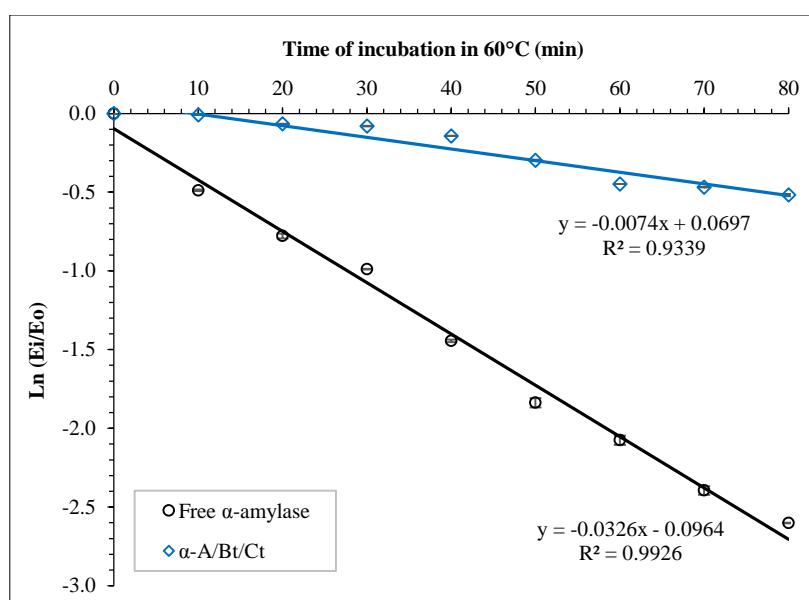


**Figure 9.** Plot of first-order inactivation rates of free  $\alpha$ -amylase and  $\alpha$ -A/Bt/Ct of *A. fumigatus* (mean  $\pm$  SD;  $n = 2$ ;  $p < 0.05$ )

**Table 5.** Half-life and  $\Delta G_i$  values of free and immobilized  $\alpha$ -amylase from *A. fumigatus* in different matrices

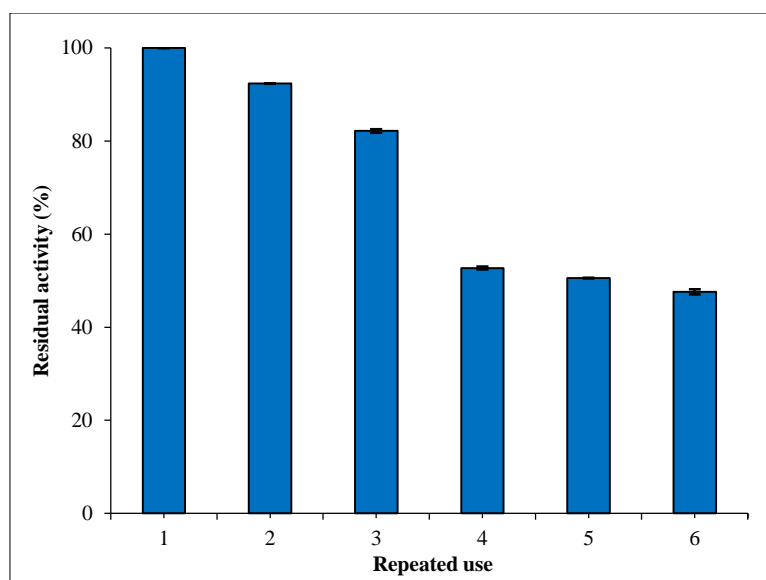
Matrix	$t_{1/2}$ (min)		$\Delta G_i$ (kJ mol $^{-1}$ )		Improved stability	Reference
	Free $\alpha$ -amylase	Immobilized $\alpha$ -amylase	Free $\alpha$ -amylase	Immobilized $\alpha$ -amylase		
Bentonite	40.53 $\pm$ 1.90	115.50 $\pm$ 5.79	104.47 $\pm$ 0.13	107.37 $\pm$ 0.14	2.9	[24]
Zeolite	38.75 $\pm$ 1.53	92.40 $\pm$ 0.00	104.35 $\pm$ 1.09	106.76 $\pm$ 0.00	2.38	[50]
Zeolite/chitosan	38.75 $\pm$ 1.53	180.03 $\pm$ 3.31	104.35 $\pm$ 1.09	108.03 $\pm$ 0.05	4.65	[25]
Bentonite/chitin	40.53 $\pm$ 1.90	154.00 $\pm$ 13.34	104.47 $\pm$ 0.13	108.17 $\pm$ 0.24	3.8	[23]
Bentonite/chitosan	21.23 $\pm$ 0.23	94.29 $\pm$ 0.91	102.68 $\pm$ 0.30	104.43 $\pm$ 0.00	4.44 $\pm$ 0.01	This study

Table 5 shows that the  $\Delta G_i$  value of  $\alpha$ -A/Bt/Ct is larger than that of free  $\alpha$ -amylase, in which the  $\Delta G_i$  value of 102.684  $\pm$  0.30 kJ mol $^{-1}$  was found for the free enzyme, while for  $\alpha$ -A/Bt/Ct the  $\Delta G_i$  value is 104.427  $\pm$  0.00 kJ mol $^{-1}$ . A higher  $\Delta G_i$  value suggests that the immobilized enzyme is a more stable enzyme and has experienced a lower thermal denaturation process. The  $\Delta G_i$  value is determined by stabilizing factors in the enzyme structure, such as hydrogen bonds and Vander Waals interactions in the enzyme's 3D structure. In contrast, the lower  $\Delta G_i$  value of free amylase reflects a spontaneous thermal denaturation process, implying that free amylase unfolds quicker than  $\alpha$ -A/Bt/Ct. If the hydrogen bonds and Vander Waals interactions in the enzyme are broken, the enzyme will lose its stabilizing power [56, 57]. The non-covalent interaction between the enzyme and the matrix in the adsorption technique protects the enzyme and strengthens its structure, preventing denaturation of the enzyme. The  $\alpha$ -A/Bt/Ct structure is more rigid, allowing the enzyme to live and settle at higher temperatures than free  $\alpha$ -amylase. This is demonstrated by the fact that the half-life ( $t_{1/2}$ ) of  $\alpha$ -A/Bt/Ct is 4.44  $\pm$  0.01 times greater than that of free  $\alpha$ -amylase. Table 5 demonstrates that the enzyme immobilized on the hybrid matrix has significantly higher stability than that immobilized on the traditional matrix. This is because the hybrid matrix protects the enzyme better than the traditional matrix, enabling the enzyme to retain higher activity.

### 3-9- Repeated Use

The immobilization technique for increasing enzyme stability offers the opportunity for repeat using of the enzyme, since the enzymes bound to specific matrices can maintain catalytic activity even after repetitive use. Figure 10 depicts the effects of repeated use of  $\alpha$ -A/Bt/Ct investigated in this study.

Table 6 compares the findings of repetitive use of  $\alpha$ -amylase immobilized on different matrices used. The process of repeated usage results in a reduction of enzyme activity. This is due to enzyme loss after repeated washing, dissolution of some of the matrix during the washing process, and denaturation of the enzymes [58]. According to Table 6, using chitosan in combination with bentonite can boost the residual activity from the repeated use process. As can be seen, the enzyme immobilized on bentonite alone was able to retain the residual activity of only 42%, while the enzyme immobilized on bentonite/chitosan was able to retain 47.61  $\pm$  0.53% residual activity. Furthermore, when chitosan is combined with bentonite, the recurrent usage of enzymes is increased as compared to bentonite/chitin. This permits the NH $_2$  group to better maintain the active group of the enzyme [58].



**Figure 10.** Repeated use of  $\alpha$ -A/Bt/Ct from *A. fumigatus* (mean  $\pm$  SD; n = 2; p < 0.05)

**Table 6.** Repeated use of immobilized enzyme in different matrices

Enzyme	Host	Matrix	Repeated use	Residual activity (%)	Reference
$\alpha$ -amylase	<i>A. fumigatus</i>	Bentonite	6	42	[24]
Maltogenic amylase	<i>B. lehensis</i> G1	Alginate	8	35	[59]
Maltogenic amylase	<i>B. lehensis</i> G1	Alginate/chitosan	8	21	[59]
$\alpha$ -amylase	<i>A. fumigatus</i>	Zeolite/chitosan	5	11	[25]
$\alpha$ -amylase	<i>A. fumigatus</i>	Bentonite/chitin	6	38	[23]
$\alpha$ -amylase	<i>A. fumigatus</i>	Bentonite/chitosan	6	47.61 $\pm$ 0.53*	This study

\* (mean  $\pm$  SD; n = 2; p < 0.05)

## 4- Conclusion

The use of bentonite/chitosan matrix as immobilization support was found to effectively improve the stability of the  $\alpha$ -amylase from *A. fumigatus*. Purified  $\alpha$ -amylase has a purity level of 19.40 times that of crude extract. The optimum adsorption conditions between enzymes and bentonite/chitosan in the acidic pH range (phosphate buffer pH 6) sustain the pH of free  $\alpha$ -amylase, minimizing enzyme activity loss. The immobilized enzyme is categorized as thermostable, as demonstrated by increasing the optimum temperature from 50 to 60°C. The immobilized amylase is then more stable than free amylase at elevated temperatures (60-80°C). Following immobilization, the  $K_M$  and  $V_{max}$  values changed significantly, in which the immobilized enzyme having a greater  $K_M$  value than that of free enzyme, suggesting a lower affinity for the substrate. As a result, the maximum rate ( $V_{max}$ ) is reduced, and a larger quantity of substrate is required. The immobilization of *A. fumigatus*  $\alpha$ -amylase on a bentonite/chitosan hybrid matrix improved its thermal stability, reusability, and characteristics. The rise in residual activity in the thermal stability test from 7.42  $\pm$  0.02 to 59.61  $\pm$  0.43, or with a ratio of around 8.04  $\pm$  0.04, demonstrated that the  $\alpha$ -amylase was protected from inactivation by the bentonite/chitosan matrix. The half-life of  $\alpha$ -amylase/bentonite/chitosan increased from 21.23  $\pm$  0.23 minutes to 94.29  $\pm$  0.91 minutes, or by 4.44  $\pm$  0.01 times when compared to free  $\alpha$ -amylase. The value of the Gibbs free energy ( $\Delta G_i$ ) increased from 102.68  $\pm$  0.30 to 104.43  $\pm$  0.00 kJ mol<sup>-1</sup>, indicating that  $\alpha$ -amylase/bentonite/chitosan was stiffer and more stable than free  $\alpha$ -amylase. The immobilized enzyme retained an activity of 47.61  $\pm$  0.53% after six successive uses, indicating that it has the ability to be used in industry. As a result, this method offers a straightforward and effective method for using bentonite/chitosan hybrids, as well as a possible utility as a matrix to support enzyme immobilization.

## 5- Declarations

### 5-1- Author Contributions

Conceptualization, Y.Y. and H.R.; methodology, Y.Y., H.R., and B.I.; software, H.R. and S.H.; validation, Y.Y., T.S., B.I., and S.H.; writing—original draft preparation, Y.Y. and H.R.; writing—review and editing, Y.Y., T.S., and S.H.; visualization, H.R.; supervision, Y.Y. and T.S.; project administration, Y.Y. and S.H.; funding acquisition, Y.Y. All authors have read and agreed to the published version of the manuscript.

### 5-2-Data Availability Statement

The data presented in this study are available in the article.

### 5-3-Funding

The authors are grateful to the Ministry of Education, Culture, Research and Technology for funding this study based on Basic Research 2023 with contract numbers 027/E5/PG.02.00.PL/2023 on 12<sup>th</sup> April 2023 and 2192/UN26.21/PN/2023 on 17th April 2023.

### 5-4-Acknowledgements

The authors acknowledged the Ministry of Education, Culture, Research, and Technology of Indonesia for assisting this study.

### 5-5-Institutional Review Board Statement

Not applicable.

### 5-6-Informed Consent Statement

Not applicable.

### 5-7-Conflicts of Interest

The authors declare that there is no conflict of interest regarding the publication of this manuscript. In addition, the ethical issues, including plagiarism, informed consent, misconduct, data fabrication and/or falsification, double publication and/or submission, and redundancies have been completely observed by the authors.

## 6- References

- [1] Farooq, M. A., Ali, S., Hassan, A., Tahir, H. M., Mumtaz, S., & Mumtaz, S. (2021). Biosynthesis and industrial applications of  $\alpha$ -amylase: a review. *Archives of Microbiology*, 203(4), 1281–1292. doi:10.1007/s00203-020-02128-y.
- [2] Jujjavarapu, S. E., & Dhagat, S. (2018). Evolutionary trends in industrial production of  $\alpha$ -amylase. *Recent Patents on Biotechnology*, 13(1), 4–18. doi:10.2174/2211550107666180816093436.
- [3] Singh, R., Kim, S. W., Kumari, A., & Mehta, P. K. (2022). An overview of microbial  $\alpha$ -amylase and recent biotechnological developments. *Current Biotechnology*, 11(1), 11–26. doi:10.2174/2211550111666220328141044.
- [4] Future Market Insights. (2022). Alpha-amylase baking enzyme market outlook (2022-2032). Future Market Insights, Newark, United States. Available online: <https://www.futuremarketinsights.com/reports/alpha-amylase-baking-enzyme-market> (accessed on March 2023).
- [5] Vachher, M., Sen, A., Kapila, R., & Nigam, A. (2021). Microbial therapeutic enzymes: A promising area of biopharmaceuticals. *Current Research in Biotechnology*, 3, 195–208. doi:10.1016/j.crbiot.2021.05.006.
- [6] Streimikyte, P., Viskelis, P., & Viskelis, J. (2022). Enzymes-assisted extraction of plants for sustainable and functional applications. *International Journal of Molecular Sciences*, 23(4), 2359. doi:10.3390/ijms23042359.
- [7] Barzee, T. J., Cao, L., Pan, Z., & Zhang, R. (2021). Fungi for future foods. *Journal of Future Foods*, 1(1), 25–37. doi:10.1016/j.jfutfo.2021.09.002.
- [8] Blaga, A. C., Cașcaval, D., & Galaction, A. I. (2022). Improved production of  $\alpha$ -amylase by *Aspergillus terreus* in presence of oxygen-vector. *Fermentation*, 8(6), 271. doi:10.3390/fermentation8060271.
- [9] Devi, R., Revathi, K., Arunagirinathan, N., & Yogananth, N. (2022). Production and optimization of  $\alpha$ -amylase from *Aspergillus ochraceus* isolated from Marakkanam Saltpans, Tamil Nadu, India. *Bulletin of Environment, Pharmacology and Life Sciences*, 1, 997-1002.
- [10] Premalatha, A., Vijayalakshmi, K., Shanmugavel, M., & Rajakumar, G. S. (2023). Optimization of culture conditions for enhanced production of extracellular  $\alpha$ -amylase using solid-state and submerged fermentation from *Aspergillus tamarii* MTCC5152. *Biotechnology and Applied Biochemistry*, 70(2), 835–845. doi:10.1002/bab.2403.
- [11] Beltagy, E. A., Abouelwafa, A., & Barakat, K. M. (2022). Bioethanol production from immobilized amylase produced by marine *Aspergillus flavus* AUMC10636. *Egyptian Journal of Aquatic Research*, 48(4), 325–331. doi:10.1016/j.ejar.2022.02.003.
- [12] Sidar, A., Voshol, G. P., Vijgenboom, E., & Punt, P. J. (2023). Novel design of an  $\alpha$ -amylase with an N-terminal CBM20 in *Aspergillus niger* improves binding and processing of a broad range of starches. *Molecules*, 28(13), 5033. doi:10.3390/molecules28135033.

- [13] Marengo, M., Pezzilli, D., Gianquinto, E., Fissore, A., Oliaro-Bosso, S., Sgorbini, B., Spyraakis, F., & Adinolfi, S. (2022). Evaluation of porcine and *Aspergillus oryzae*  $\alpha$ -amylases as possible model for the human enzyme. *Processes*, 10(4), 780. doi:10.3390/pr10040780.
- [14] Yandri, Y., Nurmala, N., Suhartati, T., Satria, H., & Hadi, S. (2022). The stability increase of  $\alpha$ -amylase enzyme from *Aspergillus fumigatus* using dimethyladipimide. *Physical Sciences Reviews*, 8(10), 3655-3664. doi:10.1515/psr-2021-0138.
- [15] Fang, W., & Latgé, J.-P. (2018). Microbe profile: *Aspergillus fumigatus*: A saprotrophic and opportunistic fungal pathogen. *Microbiology*, 164(8), 1009–1011. doi:10.1099/mic.0.000651.
- [16] Rathnakumar, K., Kalaivendan, R. G. T., Eazhumalai, G., Raja Charles, A. P., Verma, P., Rustagi, S., Bharti, S., Kothakota, A., Siddiqui, S. A., Manuel Lorenzo, J., & Pandiselvam, R. (2023). Applications of ultrasonication on food enzyme inactivation—recent review report (2017–2022). *Ultrasonics Sonochemistry*, 96, 106407. doi:10.1016/j.ultsonch.2023.106407.
- [17] Mohamad, N. R., Marzuki, N. H. C., Buang, N. A., Huyop, F., & Wahab, R. A. (2015). An overview of technologies for immobilization of enzymes and surface analysis techniques for immobilized enzymes. *Biotechnology & Biotechnological Equipment*, 29(2), 205–220. doi:10.1080/13102818.2015.1008192.
- [18] Zhang, Y., Ge, J., & Liu, Z. (2015). Enhanced activity of immobilized or chemically modified enzymes. *ACS Catalysis*, 5(8), 4503–4513. doi:10.1021/acscatal.5b00996.
- [19] Oliveira, F. L., de S. França, A., de Castro, A. M., Alves de Souza, R. O. M., Esteves, P. M., & Gonçalves, R. S. B. (2020). Enzyme immobilization in covalent organic frameworks: Strategies and applications in biocatalysis. *ChemPlusChem*, 85(9), 2051–2066. doi:10.1002/cplu.202000549.
- [20] Zdarta, J., Meyer, A. S., Jesionowski, T., & Pinelo, M. (2018). A general overview of support materials for enzyme immobilization: Characteristics, properties, practical utility. *Catalysts*, 8(2), 92. doi:10.3390/catal8020092.
- [21] Dong, H., Li, Y., Li, J., Sheng, G., & Chen, H. (2013). Comparative study on lipases immobilized onto bentonite and modified bentonites and their catalytic properties. *Industrial & Engineering Chemistry Research*, 52(26), 9030–9037. doi:10.1021/ie4001986.
- [22] Mo, H., & Qiu, J. (2020). Preparation of chitosan/magnetic porous biochar as support for cellulase immobilization by using glutaraldehyde. *Polymers*, 12(11), 2672. doi:10.3390/polym12112672.
- [23] Tiarsa, E. R., Yandri, Y., Suhartati, T., Satria, H., Irawan, B., & Hadi, S. (2022). The stability improvement of *Aspergillus fumigatus*  $\alpha$ -amylase by immobilization onto chitin-bentonite hybrid. *Biochemistry Research International*, 2022, 5692438. doi:10.1155/2022/5692438.
- [24] Yandri, Y., Tiarsa, E. R., Suhartati, T., Satria, H., Irawan, B., & Hadi, S. (2022). The stability improvement of  $\alpha$ -amylase enzyme from *Aspergillus fumigatus* by immobilization on a bentonite matrix. *Biochemistry Research International*, 2022, 3797629. doi:10.1155/2022/3797629.
- [25] Yandri, Y., Ropingi, H., Suhartati, T., Hendri, J., Irawan, B., & Hadi, S. (2022). The effect of zeolite/chitosan hybrid matrix for thermal-stabilization enhancement on the immobilization of *Aspergillus fumigatus*  $\alpha$ -amylase. *Emerging Science Journal*, 6(3), 505–518. doi:10.28991/ESJ-2022-06-03-06.
- [26] Bollag, D. M., Rozycki, M. D., & Edelstein, S. J. (1996). *Protein methods* (2<sup>nd</sup> Ed.). John Wiley & Sons, Hoboken, United States.
- [27] Fuwa, H. (1954). A new method for microdetermination of amylase activity by the use of amylose as the substrate. *Journal of Biochemistry*, 41(5), 583–603. doi:10.1093/oxfordjournals.jbchem.a126476.
- [28] Eveleigh, D. E., Mandels, M., Andreotti, R., & Roche, C. (2009). Measurement of saccharifying cellulase. *Biotechnology for Biofuels*, 2(1), 21. doi:10.1186/1754-6834-2-21.
- [29] Lowry, O. H., Rosebrough, N. J., Farr, A. L., & Randall, R. J. (1951). Protein measurement with the Folin phenol reagent. *The Journal of Biological Chemistry*, 193(1), 265–275. doi:10.1016/s0021-9258(19)52451-6.
- [30] Yang, Z., Domach, M., Auger, R., Yang, F. X., & Russell, A. J. (1996). Polyethylene glycol-induced stabilization of subtilisin. *Enzyme and Microbial Technology*, 18(2), 82–89. doi:10.1016/0141-0229(95)00073-9.
- [31] Kazan, D., Ertan, H., & Erarslan, A. (1997). Stabilization of *Escherichia coli* penicillin G acylase against thermal inactivation by cross-linking with dextran dialdehyde polymers. *Applied Microbiology and Biotechnology*, 48(2), 191–197. doi:10.1007/s002530051037.
- [32] Planchot, V., & Colonna, P. (1995). Purification and characterization of extracellular alpha-amylase from *Aspergillus fumigatus*. *Carbohydrate Research*, 272(1), 97–109. doi:10.1016/0008-6215(95)00035-R.
- [33] Ahmed, K., Valeem, E. E., Khan, M. A., & Qamar-Ul-Haq. (2015). Biosynthesis of alpha amylase from *Aspergillus fumigatus* (fresenius 1863) in submerged fermentation. *Pakistan Journal of Biotechnology*, 12(2), 89–92.

- [34] Akhter, M., Hossain, M. T., & Anwar, M. (2013). Factors responsible for production of amylases from *Aspergillus fumigatus* Fresenius. *Chittagong University Journal of Biological Sciences*, 11–20. doi:10.3329/cujbs.v3i1.13402.
- [35] Chen, Y., Huang, R., Zhu, C., Wu, D., Sun, Y., He, Y., & Ye, W. (2014). Adsorptive removal of La(III) from aqueous solutions with 8-hydroxyquinoline immobilized GMZ bentonite. *Journal of Radioanalytical and Nuclear Chemistry*, 299(1), 665–674. doi:10.1007/s10967-013-2768-4.
- [36] Chen, X., Wang, J., Wang, S., Ma, F., Chen, X., & Li, J. (2015). Effect of solution properties on the interaction of <sup>90</sup>Sr(II) with GMZ bentonite. *Korean Journal of Chemical Engineering*, 32(11), 2264–2272. doi:10.1007/s11814-015-0045-7.
- [37] Belousov, P., Semenkova, A., Egorova, T., Romanchuk, A., Zakusin, S., Dorzhieva, O., Tyupina, E., Izosimova, Y., Tolpeshta, I., Chernov, M., & Krupskaya, V. (2019). Cesium sorption and desorption on glauconite, bentonite, zeolite, and diatomite. *Minerals*, 9(10), 625. doi:10.3390/min9100625.
- [38] Tabak, A., Afsin, B., Caglar, B., & Koksall, E. (2007). Characterization and pillaring of a Turkish bentonite (Resadiye). *Journal of Colloid and Interface Science*, 313(1), 5–11. doi:10.1016/j.jcis.2007.02.086.
- [39] Zvezdova, D. (2010). Synthesis and characterization of chitosan from marine sources in Black Sea. *Annual Proceedings, "Angel Kanchev" University of Ruse*, 49(9.1), 65–69.
- [40] Chen, C., Gao, Z., Qiu, X., & Hu, S. (2013). Enhancement of the controlled-release properties of chitosan membranes by crosslinking with suberoyl chloride. *Molecules*, 18(6), 7239–7252. doi:10.3390/molecules18067239.
- [41] Augustine, M., Madhusudhanan, D. T., & Velayudhan, M. P. (2023). Thermal deactivation studies of alpha-amylase immobilized onto core-shell structured aniline formaldehyde crosslinked polyaniline magnetic nanocomposite. *Biotechnology & Biotechnological Equipment*, 37(1), 273–285. doi:10.1080/13102818.2023.2182150.
- [42] Wang, Z., Ren, D., Cheng, Y., Zhang, X., Zhang, S., & Chen, W. (2022). Immobilization of laccase on chitosan functionalized halloysite nanotubes for degradation of Bisphenol A in aqueous solution: Degradation mechanism and mineralization pathway. *Heliyon*, 8(7), 9919. doi:10.1016/j.heliyon.2022.e09919.
- [43] Madera-Santana, T. J., Herrera-Méndez, C. H., & Rodríguez-Núñez, J. R. (2018). An overview of the chemical modifications of chitosan and their advantages. *Green Materials*, 6(4), 131–142. doi:10.1680/jgrma.18.00053.
- [44] Alnadari, F., Xue, Y., Zhou, L., Hamed, Y. S., Taha, M., & Foda, M. F. (2020). Immobilization of  $\beta$ -glucosidase from *Thermatoga maritima* on chitin-functionalized magnetic nanoparticle via a novel thermostable chitin-binding domain. *Scientific Reports*, 10(1), 1–12. doi:10.1038/s41598-019-57165-5.
- [45] Yandri, Y., Tiarsa, E. R., Suhartati, T., Irawan, B., & Hadi, S. (2023). Immobilization and stabilization of *Aspergillus fumigatus*  $\alpha$ -amylase by adsorption on a chitin. *Emerging Science Journal*, 7(1), 77–89. doi:10.28991/ESJ-2023-07-01-06.
- [46] Klapiszewski, L., Zdarta, J., & Jesionowski, T. (2018). Titania/lignin hybrid materials as a novel support for  $\alpha$ -amylase immobilization: A comprehensive study. *Colloids and Surfaces B: Biointerfaces*, 162, 90–97. doi:10.1016/j.colsurfb.2017.11.045.
- [47] Bodakowska-Boczniewicz, J., & Garncarek, Z. (2019). Immobilization of naringinase from *penicillium decumbens* on chitosan microspheres for debittering grapefruit juice. *Molecules*, 24(23), 4234. doi:10.3390/molecules24234234.
- [48] Tincu, C. E., Bouhadiba, B., Atanase, L. I., Stan, C. S., Popa, M., & Ochiuz, L. (2023). An accessible method to improve the stability and reusability of porcine pancreatic  $\alpha$ -amylase via immobilization in gellan-based hydrogel particles obtained by ionic cross-linking with  $Mg^{2+}$  ions. *Molecules*, 28(12), 4695. doi:10.3390/molecules28124695.
- [49] Ahmed, N. E., El Shamy, A. R., & Awad, H. M. (2020). Optimization and immobilization of amylase produced by *Aspergillus terreus* using pomegranate peel waste. *Bulletin of the National Research Centre*, 44(1), 109. doi:10.1186/s42269-020-00363-3.
- [50] Yandri, Y., Ropingi, H., Suhartati, T., Irawan, B., & Hadi, S. (2023). Immobilization of  $\alpha$ -amylase from *Aspergillus fumigatus* using adsorption method onto zeolite. *Physical Sciences Reviews*, 1–12. doi:10.1515/psr-2022-0258.
- [51] Nazarova, E. A., Yushkova, E. D., Ivanets, A. I., Prozorovich, V. G., Krivoshapkin, P. V., & Krivoshapkina, E. F. (2021).  $\alpha$ -Amylase immobilization on ceramic membranes for starch hydrolysis. *Starch - Stärke*, 74(1), 1–9. doi:10.1002/star.202100017.
- [52] Kaushal, J., Seema, Singh, G., & Arya, S. K. (2018). Immobilization of catalase onto chitosan and chitosan–bentonite complex: A comparative study. *Biotechnology Reports*, 18, 258. doi:10.1016/j.btre.2018.e00258.
- [53] Califano, V., & Costantini, A. (2020). Immobilization of cellulolytic enzymes in mesostructured silica materials. *Catalysts*, 10(6), 706. doi:10.3390/catal10060706.
- [54] Zhang, H., Nie, M., Gu, Z., Xin, Y., Zhang, L., Li, Y., & Shi, G. (2023). Preparation of water-insoluble lignin nanoparticles by deep eutectic solvent and its application as a versatile and biocompatible support for the immobilization of  $\alpha$ -amylase. *International Journal of Biological Macromolecules*, 249, 125975. doi:10.1016/j.ijbiomac.2023.125975.

- [55] Yandri, Y., Suhartati, T., Satria, H., Widyasmara, A., & Hadi, S. (2020). Increasing stability of  $\alpha$ -amylase obtained from *Bacillus subtilis* ITBCCB148 by immobilization with chitosan. *Mediterranean Journal of Chemistry*, 10(2), 155–161. doi:10.13171/mjc10202002131126ysh.
- [56] Wu, L., Wu, S., Xu, Z., Qiu, Y., Li, S., & Xu, H. (2016). Modified nanoporous titanium dioxide as a novel carrier for enzyme immobilization. *Biosensors and Bioelectronics*, 80, 59–66. doi:10.1016/j.bios.2016.01.045.
- [57] Dhiman, S., Srivastava, B., Singh, G., Khatri, M., & Arya, S. K. (2020). Immobilization of manganese on sodium alginate-grafted- $\beta$ -cyclodextrin: An easy and cost effective approach for the improvement of enzyme properties. *International Journal of Biological Macromolecules*, 156, 1347–1358. doi:10.1016/j.ijbiomac.2019.11.175.
- [58] Yandri, Susanti, D., Suhartati, T., & Hadi, S. (2012). Immobilization of  $\alpha$ -amylase from locale bacteria isolate *Bacillus subtilis* ITBCCB148 with carboxymethyl cellulose (CM-Cellulose). *Modern Applied Science*, 6(3), 81–86. doi:10.5539/mas.v6n3p81.
- [59] Muhammad Firdaus Kumar, N. K., Meng, C. C., Manas, N. H. A., Ahmad, R. A., Mohd Fuzi, S. F. Z., Rahman, R. A., & Md Illias, R. (2022). Immobilization of maltogenic amylase in alginate-chitosan beads for improved enzyme retention and stability. *Malaysian Journal of Fundamental and Applied Sciences*, 18(1), 43–51. doi:10.11113/MJFAS.V18N1.2381.